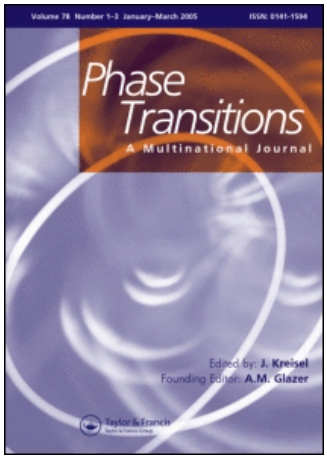

Phase Transitions
A Multinational Journal
Publication details, including instructions for authors and subscription information:
http://www.informaworld.com/smpp/title~content=t713647403

High-temperature phase transitions in the improper ferroelectric KIO_3

M. M. Abdel-Kader [a]; F. El-Kabbany [a]; H. Naguib [a]; W. M. Gamal [a]
[a] Faculty of Science, Department of Physics, Cairo University, Giza, Egypt

Online Publication Date: 01 January 2008
To cite this Article: Abdel-Kader, M. M., El-Kabbany, F., Naguib, H. and Gamal, W. M. (2008) 'High-temperature phase transitions in the improper ferroelectric KIO_3', Phase Transitions, 81:1, 29 - 41
To link to this article: DOI: 10.1080/01411590701461262
URL: http://dx.doi.org/10.1080/01411590701461262

Phase Transitions,
Vol. 81, No. 1, January 2008, 29–41

High-temperature phase transitions in the improper ferroelectric KIO_3

M. M. ABDEL-KADER*, F. EL-KABBANY, H. NAGUIB and W. M. GAMAL

Faculty of Science, Department of Physics, Cairo University, Giza, Egypt

(*Received 18 March 2007; in final form 21 May 2007*)

The ac conductivity (σ_{ac}) and dielectric permittivity (ε) are determined in the temperature range $300\,K < T < 520\,K$ at some selected frequencies (0.5–10 kHz) for the polycrystalline samples of KIO_3 compound. The results indicated that the compound behaves as an improper ferroelectric and undergoes a ferroelectric phase transition from a high temperature rhombohedral phase I to a low temperature monoclinic phase II at $T_c = (486 \pm 1)\,K$. A second structural phase transition was observed around 345 K. The conductivity varies with temperature range and for $T > 428\,K$ intrinsic conduction prevails. Different activation energies in the different temperature regions were calculated. The frequency dependence of $\sigma(\omega)$ was found to follow the universal dynamic response $[\sigma(\omega) \propto (\omega)^{s(T)}]$. The thermal behaviour of the frequency exponent $s(T)$ suggests the hopping over the barrier model rather than the quantum mechanical tunneling model for the conduction mechanism.

Keywords: Improper ferroelectrics; Electric permittivity; Electric conductivity; Phase transition; KIO_3

1. Introduction

The alkali halates form a class of compounds of the general molecular formula MXO_3 where M is an alkali element or group ($M = H$, Li, Cs, Rb, Na, K ... and/or NH_4) and X stands for halogen atom (X = Cl, Br, and I). Some members of this series possess interesting properties such as pyroelectric, piezoelectric, and nonlinear optical properties [1–5].

For the chlorate compounds of this series, there is, for example, the $KClO_3$ compound which undergoes a structural phase transition associated with a minor change in the atomic positions at 545 K [6, 7]. Probable ferroelastic properties of this compound were also investigated [8]. On the other hand, no structural phase transition were detected in the $KBrO_3$ compound [7]. Furthermore, the elastic and dynamic piezoelectric properties were studied [9].

*Corresponding author. Email: m_m_abdelkader@yahoo.com

Phase Transitions
ISSN 0141-1594 print/ISSN 1029-0338 online © 2008 Taylor & Francis
http://www.tandf.co.uk/journals
DOI: 10.1080/01411590701461262

Regarding the iodate compounds of this series and from the crystal structure point of view, in general, it was found that iodates with large ions such as Cs, Rb, and K possess perovskite like structure with distorted octahedral coordination of I. Those with smaller ions like, H, Li, and Na show a differing structure in which the typical octahedral framework of the perovskite is lacking [10]. In addition to the determination of the crystal structure of some members of iodate compounds, their physico-chemical properties were also investigated. For example, the sequences of phase transitions of $LiIO_3$ have been extensively investigated by different techniques [1, 11–13].

For potassium iodate, KIO_3, which is under current investigation in this article, an earlier report concerning successive phase transitions, based on Nuclear Quadrupole Resonance (NQR) was given by Herlach [14]; accordingly at atmospheric pressure, the compound undergoes successive phases with temperature change, as indicated below

$$\mathrm{V} \xrightarrow{83\,\mathrm{K}} \mathrm{IV} \underset{263\,\mathrm{K}}{\overset{255\,\mathrm{K}}{\rightleftharpoons}} \mathrm{III} \xrightarrow{343\,\mathrm{K}} \mathrm{II} \xrightarrow{485\,\mathrm{K}} \mathrm{I}$$

and all phases except I have been reported to be ferroelectric [14]. Furthermore, preliminary investigation of some physical properties was carried out [15–17]. Moreover, a review of crystal structures and phase transitions up to 1971 has been summarized by Crane [18].

On the other hand a single-crystal X-ray structure has been performed by Kalinin *et al.* [19] but the structure has been faced with some problems.

According to Kasatani *et al.* [20] a single crystal structure analysis for KIO_3 is difficult because of the complicated domain structure of various kinds, for example ferroelectric and/or ferroelastic domains. The second difficulty arises from pseudosymmetry as discussed by Lucas [21]. To avoid these problems and hence to obtain an accurate structure, two techniques were adopted. The first one is the high-resolution neutron powder diffraction profile and was used by Lucas [21] for the determination of the room-temperature phase (phase III) and also the high temperature phase (phase I) [22]. The second technique is based on the MEM/Rietveld analysis from high-energy synchrotone X-ray powder diffraction and was used to determine the structure of phase I [20].

Regarding the thermal properties, Loiacono *et al.* [6] examined the thermal characterization of KIO_3 in the temperature range 250–600 K by using Perkin-Elmr DSC. Two transition temperatures were detected by this technique ($T_1 = T_c \approx 487$ K and $T_2 = 345$ K) corresponding to phase transitions I–II and II–III, respectively.

For the optical properties and, according to somewhat recent work [23], the KIO_3 single crystal was found to be an excellent non-linear optical material. Its non-linear optical coefficient is larger than those of $KH_2\,PO_4$ (KDP), BaB_2O_4 (BBO), and $LiBrO_5$ (LBO) which are well-known double frequency materials[1] in ultraviolet wavelength [23]. Furthermore, the piezoelectric effects and elastic properties of single crystals of KIO_3 were investigated by Haussühl *et al.* [24]. They found that the static piezoelectric constants are about 50 times larger than

[1] Type of non-linear optical materials and can be used to produce optical second harmonic generation.

those of the α-quartz. Their results indicated also the existence of a second order ferroelastic phase transition at 345.6 K (72.6°C). Similar work was reported by Maeda *et al*. [25].

Although the phase transitions of KIO_3 are known, the mechanism governing the transitions has not been well understood [18, 25]. One of the main reasons of this discrepancy is the lack of the accurate crystal structures of different phases except for phase I. Unfortunately, some interpretation of the previous work is still speculative. It was considered in the previous work that KIO_3 is a usual member of the ABO_3 ferroelectrics where the I and O atoms exist as IO_6 octahedron. The recent picture, as obtained from the crystal structures [19–22], indicated that the I and O atoms exist as IO_3 rather than the complex IO_6. On the other hand the authors of a recent article [26] of Raman scattering from KIO_3 single crystals, suggested the existence of transit incommensurate phase just above the phase transition I–II. Also, they ascribed the crystals to improper ferroelectrics.

To the best of our knowledge there is no reported data on the ac conductivity and permittivity of polycrystalline KIO_3 compound in the form of powder. In the present work we decided to study some of the electrical properties of this compound and to see whether or not the phase transitions are reflected in the temperature-dependence measurements of these parameters. Such a study is a part of our research program concerning possible phase transitions and the change in the conduction mechanism in some organic, inorganic, and complexes [27–30] through the study of their electrical properties.

It is known that the measured complex dielectric permittivity $\varepsilon^*(\omega)$ can be analyzed into the real part $\varepsilon'(\omega)$ and the imaginary part $\varepsilon''(\omega)$ through the equation:

$$\varepsilon^*(\omega) = \varepsilon'(\omega) + i\varepsilon''(\omega). \tag{1}$$

Also the total measured ac conductivity $\sigma_{tot}(\omega)$ at a given angular frequency (ω) for a wide class of dielectric materials shows a dispersion behaviour through its dependence on (ω)

$$\sigma_{tot}(\omega) = \sigma(0) + \sigma(\omega) \tag{2}$$

$$= \sigma(0) + A\omega^{s(T)}. \tag{3}$$

Equation (3) is called universal dynamic response or the power law [31–34], $\sigma(0)$ is the dc conductivity, and A and s are characteristic parameters, which are temperature-dependent. Of particular interest is the frequency exponent s whose value lies in the range $0 < s < 1$. The exponent s is a measure of the degree of interaction with the environment.

2. Experimental

The material used in the present work was supplied by BDH chemicals Ltd. For electrical measurements, the polycrystalline samples were pressed under a suitable pressure; to form discs or pellets of about 1 cm diameter and 1.5–2 mm thickness. Air-dry conducting silver paint was supplied by (Electrolube Ltd, UK).

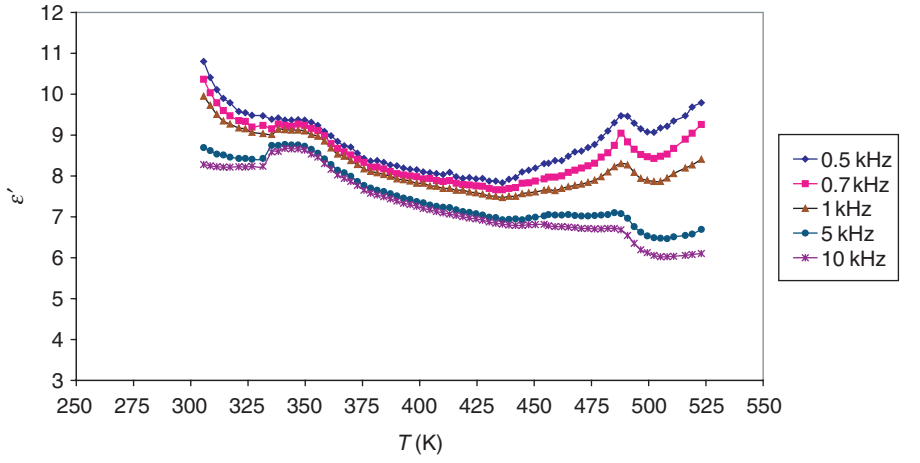

Figure 1. Temperature and frequency dependence of the real part (ε') of the dielectric permittivity.

A sample holder with brass electrodes was specially designed to fit the measurements, the temperature of the sample was measured by means of a thermocouple whose junction is inserted just to touch the sample. The terminal of the thermocouple was connected to a digital temperature system. A computerized LCR bridge was used for the measurements of the ac conductivity and dielectric permittivity at some selected frequencies.

Data were collected on at least four samples and the results were found to be quite consistent and reproducible. According to reference [6], the thermal hysteresis is found to be 1 K so data were obtained on heating runs only.

3. Results

3.1. *Relative permittivity*

The variation of the real part ε' of the electric permittivity as a function of temperature ($300\,\mathrm{K} < T < 520\,\mathrm{K}$) at some selected frequencies (0.5–10 kHz) is shown in figure 1. In general, and for a given temperature, the value of ε' decreases with increasing frequency. Regarding the features of this plot, one can identify two regions (a and b) according to the temperature range. Region (a) ($300\mathrm{K} < T < 425\,\mathrm{K}$) is characterized by the existence of a broad peak with its maximum value at ≈343–345 K. As the temperature exceeds ≈360 K, the value of ε' starts to decrease up to a temperature of ≈425 K. In region (b) ($425\,\mathrm{K} < T < 520\,\mathrm{K}$), and as the temperature approaches ≈428 K, the value of ε' starts to increase suddenly at a fast rate up to the pre-transition temperature. Beyond which a sharp peak, relative to the previous one, is observed at ≈487 K. This description holds for the low frequency range (0.5 kHz–1 kHz). However, for higher frequency range (5–10 kHz), the same trend is also observed but the rate of change of ε' is somewhat slower than expected.

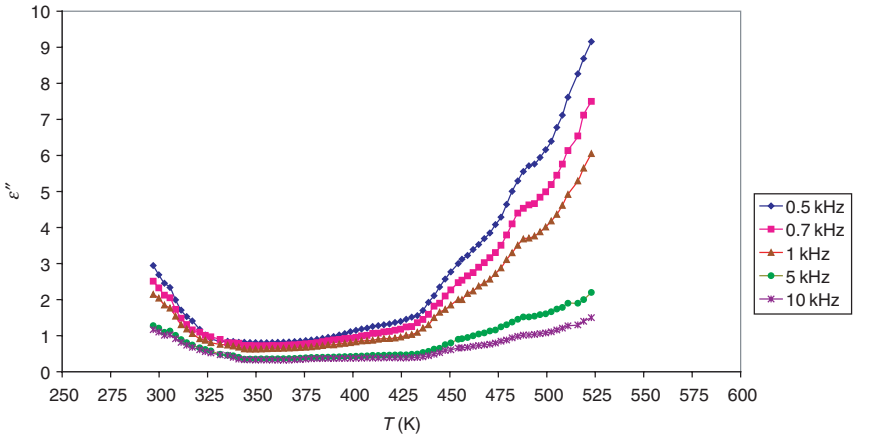

Figure 2. Variation of the imaginary part (ε'') of the dielectric permittivity with temperature measured at different frequencies.

Figure 2 shows the temperature and frequency dependence of the imaginary part ε'' of the permittivity. Here again, the value of ε'' decreases with increasing frequency. To describe the general trend of this plot, we consider two regions (a) and (b) according to the temperature range. In region (a) ($300\,\mathrm{K} < T < 425\,\mathrm{K}$), and for the low frequency range, the value of ε'' decreases with increasing frequency. The value of ε'' starts to decrease with increasing temperature up to ≈343–345 K) where the value of ε'' reaches its minimum value for each frequency. Beyond the mentioned temperature, the value of ε'' becomes slightly temperature-independent up to ≈420 K. In region (b) ($425\,\mathrm{K} < 550\,\mathrm{K}$) and beyond a temperature of 428 K, the value of ε'' starts to increase rapidly up to the pre-transition temperature. A close look at the plot indicates the existence of a shoulder at ≈487 K beyond which a continuous increase in the value of ε'' with the elevation of temperature is observed. For high frequency range (5–10 kHz) the same behaviour is observed but the rate of change of ε'' with temperature is less pronounced as compared with region (a).

The frequency dependence of ε'' plotted as ε'' versus $\ell\mathrm{n}(f)$ at different temperatures is shown in figure 3. The common feature of this plot is the observed decrease in the value of ε'' as the frequency increases. Also, the graph indicates that the dispersion increases with increasing temperature and decreasing frequency which is a typical behaviour of the dielectric material.

Figure 4 shows the variation of tan δ (permittivity loss) with temperature in the range $300\,\mathrm{K} < T < 520\,\mathrm{K}$ at selected frequencies 0.5–10 kHz. A similar behaviour to that of ε''*versus* T is observed, namely a slight decrease in the value of tan δ as the temperature increases up to ≈345 K and beyond which it begins to increase at a slow rate. However, the dispersion takes place at ≈428 K and the rate of increase of tan δ with temperature becomes faster. The plot reflects also the transition temperatures discussed previously.

3.2. *Electrical resistivity (ρ)*

The thermal variation of ρ (measured in Ω m) as a function of both the temperature and frequency is shown in figure 5. In general, and for a given temperature the value

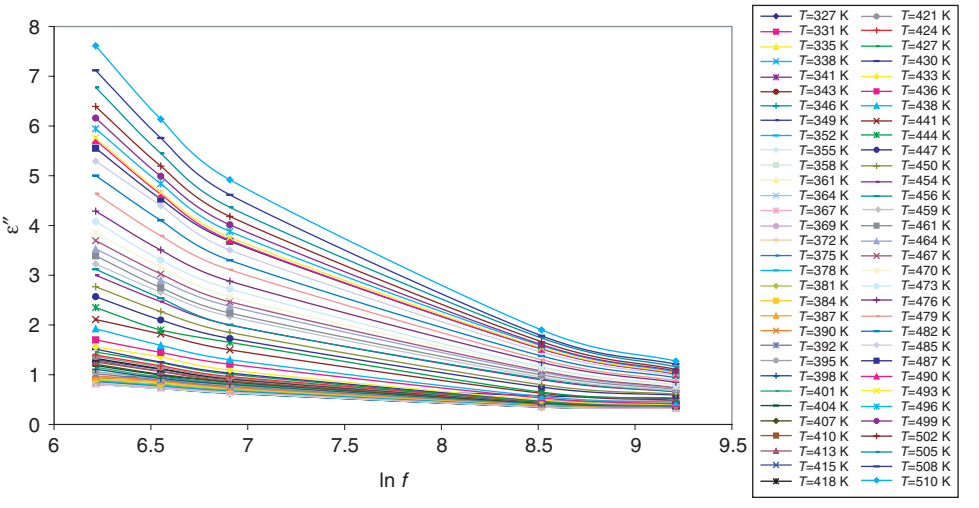

Figure 3. ε'' *vs.* $\ell n(f)$ at different temperatures.

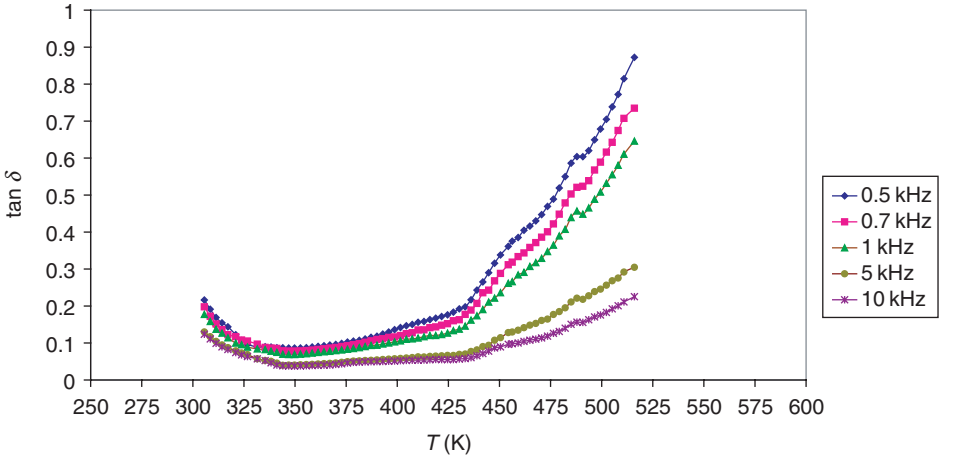

Figure 4. Temperature dependence of tan δ measured at different frequencies.

of ρ decreases with increasing the frequency. On the other hand, for a given frequency in the range (0.5–1 kHz), there is a continuous increase in the value of ρ as the temperature increases up to ≈343–345 K, where the maximum value of ρ is reached, and then starts to decrease at a very slow rate up to ≈340 K. However, as the temperature exceeds ≈372 K the rate of the decrease of ρ with temperature becomes faster and a kink or a shoulder is formed around ≈428 K. Beyond this temperature a continuous decrease in the value of ρ is observed till a dip is formed at ≈487 K. Similar behaviour was observed for high frequency range (5–10 kHz) but the rate of the change of ρ with temperature is slow in comparison with the low frequency range.

From the previous description and analysis of the data it seems likely that the transition temperatures (486 ± 1) K and (345 ± 2) K corresponding to the phase transitions I–II and II–III, respectively.

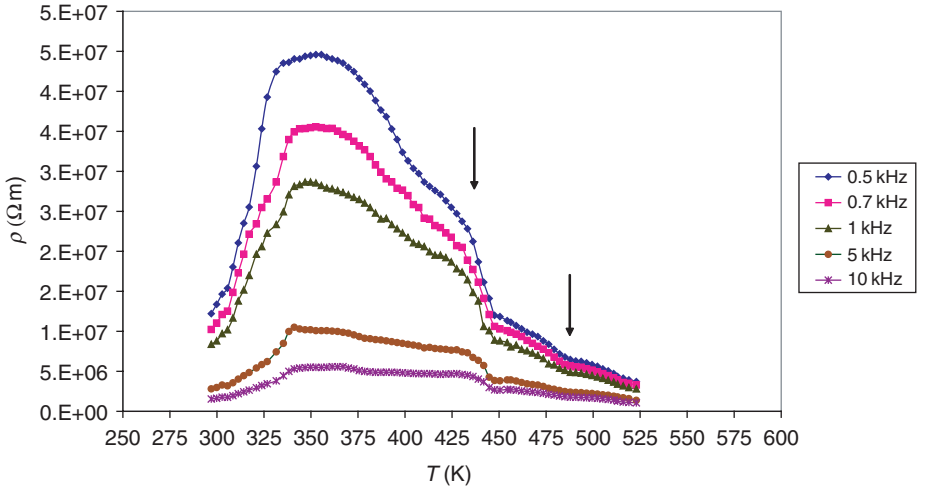

Figure 5. The relation between the resistivity (ρ) and the absolute temperature T.

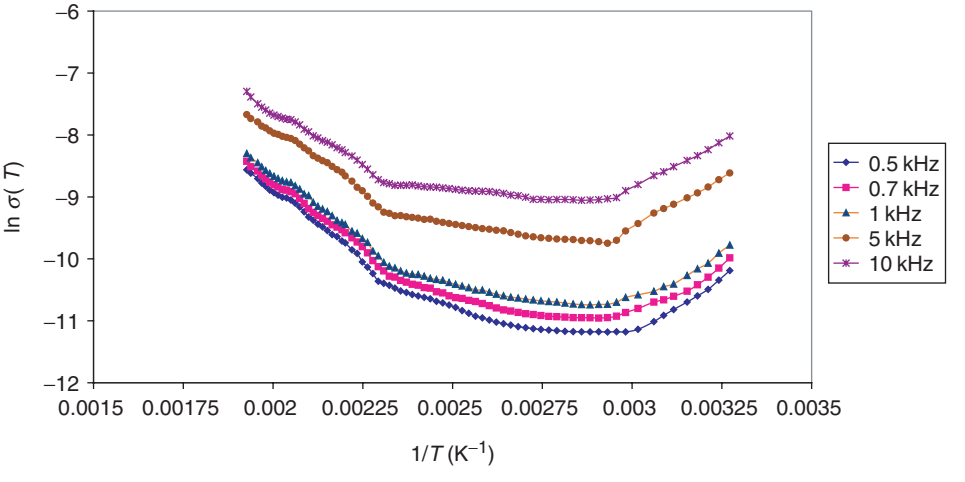

Figure 6. Variation of $\ell n\,\sigma(T)$ *vs.* $1/T$.

3.3. *Ac conductivity (σ_{ac})*

3.3.1. Temperature dependence. The conductivity data usually presented according to Arrhenous relation $\sigma(T) = \sigma_o e^{-E/kT}$. Figure 6 shows the plot of $\ln\sigma(T)$ *versus* $1/T$. One can identify four regions (a), (b), (c) and (d) according to the temperature range. Starting with region (c) ($343\,K < T < 427\,K$), the conductivity shows a weak temperature dependence but is frequency dependent. This behaviour reflects extrinsic type conduction. The activation energy is very small ≈ 0.1 eV at $f = 1$ kHz.

In region (b) ($430\,K < T < 479\,K$), the conductivity is thermally activated and the activation energy E_a slightly frequency-dependent ($E_b \approx 0.39$ eV at $f = 1$ kHz). It seems likely that this range of temperature is characterized by intrinsic conduction. The break appearing at $\approx 430\,K$ ($1/T \approx 0.0023\,K^{-1}$) reflects the change in conduction mechanism.

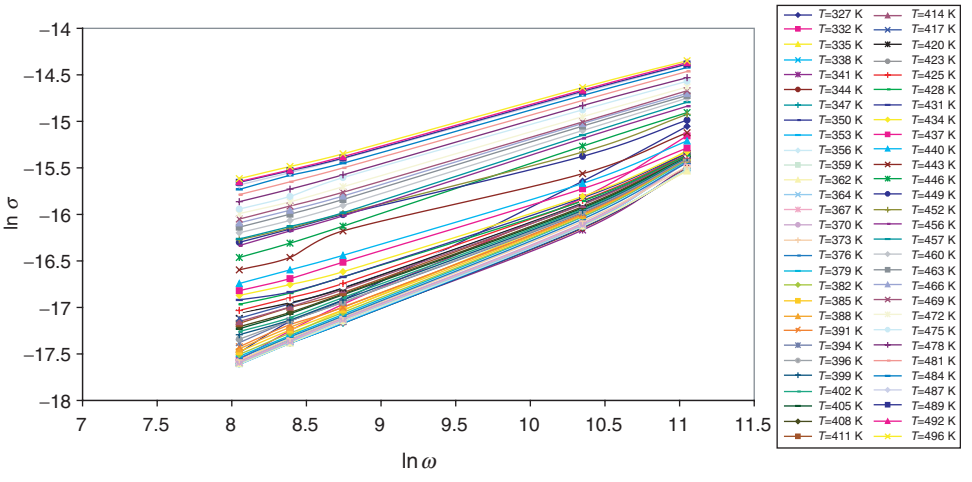

Figure 7. Double logarithmic plot: (ℓn σ *vs.* ℓn ω).

For region (a), which lies in the paraelectric phase, the conductivity is still thermally activated and the intrinsic conduction may also continue in this region. The number of data points is somewhat limited, the slope of the each line yield the value of the activation energy ($E_a = 0.48$ eV at $f = 1$ kHz). The shoulder appears at $\approx$487 K ($1/\mathrm{T} \approx 0.00205\,\mathrm{K}^{-}1$) representing the ferroelectric phase transition.

Regarding the kink between (c) and (d), which is due to the phase transition at $\approx$345 K, it is to be noted that the activation energy of region (d) is frequency-dependent and of a negative value. On the average $\mathrm{Ed} \approx |0.28|$ eV. at $f = 1$ kHz.

3.3.2. Frequency dependence. The dependence of σ_{ac} on the frequency at different temperatures in the double logarithmic representation ($\ln\sigma$ *vs.* $\ln\omega$) is shown in figure 7. The general trend of the plot shown follows the power law, equation (3), where straight lines of slightly different slopes are obtained.

The values of the frequency exponent (s) were calculated from the slope, ($s = \partial \ln\sigma / \partial \ln\omega$) of each line and the thermal variation of s *versus* T is shown in figure 8. The general feature of the temperature dependence of s is the continuous decreases of its value as the temperature increases. This behaviour suggests the hopping model rather than quantum mechanical tunneling (QMT). This problem will be discussed later on.

4. Discussion

The measured electrical parameters of KIO_3 compound show three anomalies at temperatures (345 ± 2) K, (428 ± 2) K, and (486 ± 1) K, respectively. This behaviour reflects some sort of phase transitions and/or change in the conduction mechanism at the mentioned temperatures. Subsequently, we shall explain the nature of each transition.

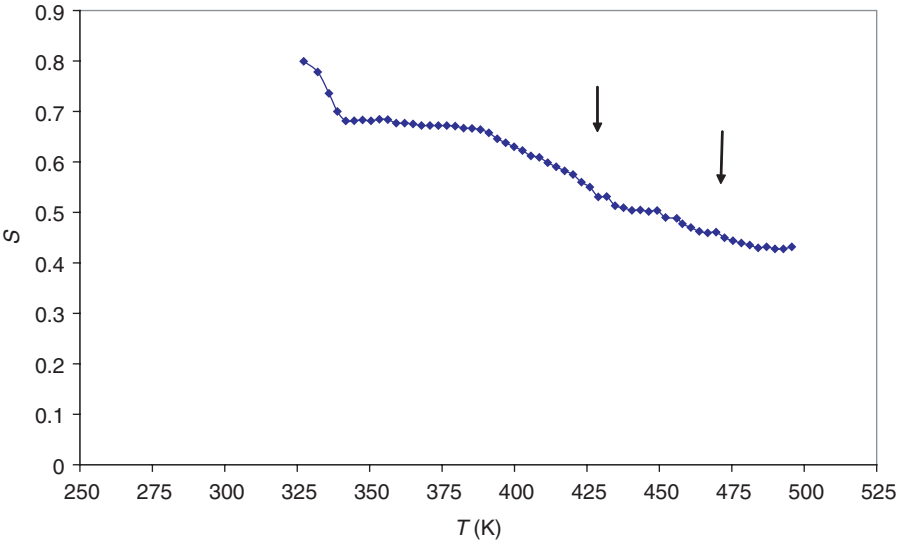

Figure 8. Temperature dependence of the frequency exponent (*s*).

The transition at (428 ± 2) K was observed in the temperature dependence measurements of some parameters such as conductivity and permittivity and has not been reflected in the heat capacity, DTA and/or DSC measurements [6]. Furthermore, the available X-ray and/or neutron diffractions data do not reveal the existence of a structural phase transition in KIO_3 at that temperature. Moreover, Yin and Lu [23] clarified that there is no new electric domains or twins produced at the region of 425 K and hence no ferroelectric phase transition exists at that temperature. Also, from their measurements of the temperature dependence of the optical axes angle (2v), Ivanov *et al.* [17] found no anomaly (i.e no detectable change in the value of 2v was observed) in the temperature regions around 425 K.

In summary, there is no evidence that confirms the existence of structural or ferroelectric phase transitions in this region. Thus we suggest that the anomaly appearing at (428 ± 2) K in the conductivity and/or permittivity plots is due to the change in the electric conduction from extrinsic below (428 ± 2) K to intrinsic above (428 ± 2) K. The activation energy in the extrinsic range is a measure of the energy required to move permanent defects (which we suggest to be an excess of HIO_3). In the intrinsic range, the conductivity is thermally activated. It is to be noted that the conductivity increases at a fast rate for $T > 428$ K; yet the order of magnitude of σ suggests highly ionic conduction but still less than superionic conduction.

The transition at (486 ± 1) K represents a ferroelectric phase transition from a high temperature paraelectric phase I (rhomhedral- $R3m$, $z = 1$) to a low temperature ferroelectric phase II (monoclinic $P\,m$, $z = 2$) at $T_c = (486 \pm 1)$ K [26, 35].

Based on (or according to) the general feature of our electrical data, one can observe the absence of the spike in the ε'–T plot, figure (1) at $T_c = (486 \pm 1)$ K, whereas ε''–T plot is characterized by the existence of only a small shoulder at T_c. It is known that, for conventional or common (proper) ferroelectric materials, the order parameter is the spontaneous polarization and the anomalies (spikes) in the dielectric properties are a direct consequence of the increased correlation in the order parameter fluctuations near T_c. This is not the case for the ferroelectric phase

transition in the present compound. Thus, based on the electrical measurements, it seems likely that, KIO_3 belongs to the second class of ferroelectrics known as improper ferroelectric where the order parameter is not the spontaneous polarization but are some physical quantities at the Brillouin zone boundary [36]. In other words, the order parameters are not proportional to the polarization [37–38]. From their investigation of the phase transition in KIO_3 single crystals, by Raman scattering, Ahart *et al*. [36] observed the similarity of the ferroelectric phase transition (I–II) in KIO_3 to that of the first improper ferroelectric namely gadolinium molybdate, $Gd_2(MoO_4)_3$ "GMO" [39]. According to Cross and Fouskova [40] the dielectric properties of GMO are essentially normal and that the spontaneous polarization is the consequence of an elastic instability giving rise to a spontaneous strain in the piezoelectric structure [40].

Since the ferroelectric phase transition represents a special class of structural phase changes, it is necessary to comment on the structural phase transformation from phase I to phase II. We concentrate our attention on the more recent refinement of the crystal structure of phase I by the MEM/Rietveld analysis [20] and also by neutron diffraction [22]. According to Kasatani *et al*. [20], the structure of phase I belongs to rhombohedral perovskite (space group $R3m$, $z = 1$, $a = 4.5137$, $\alpha = 89.210$) and the structure reveals that the shorter I–O (1.790 Å) exhibits a covalent bonding character and other I–K, K–O and longer I–O have ionic bonding. The iodine and oxygen atoms exist as IO_3^- molecules, and the spatial between IO_3^- molecules becomes weak with increasing temperature. On the other hand, based on neutron diffraction data, Byram and Lucas [22] argued that phase I belongs to rhombohedral (pseudo-cubic), non-centrosymmetric structure space group $R3$, $z = 1$, $a = 4.4973$ Å and $\alpha = 89.218$. The authors also proposed that the only structural phase transition is from the triclinic room temperature phase III to phase I. The proposed mechanism is by the displacement of K and I atoms by approximately 0.1 Å, O atoms by approximately 0.2 Å and the slightly distorted IO_3 groups in phase III becomes regular about threefold symmetry axes in phase I. As one can see, the two visions (points of view) concerning the mechanism of the structural phase transition are complement to each other, while the vision of ref. [22] deals with the descriptions of the displacement of different atoms of KIO_3 upon transition from III to I, The main feature of the other vision of ref. [20] is the weakness of the spatial correlation between IO_3^- molecules with increasing temperature.

In the present work we construct a bridge or a link between the two visions. As the temperature increases, the thermal energy (kT) gained by the KIO_3 molecules increases and, at a certain temperature ($\approx$487 K), the corresponding thermal energy may be large enough to cause such displacement of different atoms of KIO_3 as described by Lucas *et al*. [22]. This is due to the weakness of IO_3^- as suggested by Kasatani *et al*. [20] and hence the structural phase transition is observed. Another point of interest was given recently by Liu *et al*. [26]. They suggested that the structure in rhombohedral phase I observed by neutron scattering should be precursor incommensurate (INC) structure of phase transition I–II rather than a rhombohedral one with symmetry $R3$. Furthermore they add– the seemingly inconsistent descriptions of phase I of KIO_3 from neutron scattering [22] and XRD [20] can be understood easily by the proposal of INC behaviour which appears just above the phase transition I–II. They also mentioned that, with the existence of transient INC phase, the typical improper ferroelectric features of KIO_3, i.e., slight change of ε' near T_c and also the low spontaneous polarization,

can be explained. Our present electrical properties of KIO_3 agree quite well with this proposal.

The transition at (345 ± 2) K is not a ferroelectric phase transition, since the compound behaves as ferroelectrics below and above the mentioned temperature where one can observe the formation of hysteresis loops. According to Yin and Lü [23], no new electric domains and twins are produced around that temperature ($\approx$343 K) and hence no ferroelectric transformation exists.

Regarding our electrical data, this transition is reflected as a broad peak in the ε'–T plot (figure 1) and only a change in the slope at this temperature in the ε''–T graph (figure 2). However, this transition is more pronounced in the ρ-T plot and/or $\ln \sigma(\mathrm{T})$ *versus* $1/T$ (figures 3 and 4). Another point of interest in this respect, which supports and confirms the present work, is the thermal analysis if KIO_3 single crystals given by Loiacono and Jacco in ref. [6]. They found a small value of the latent heat ΔH and also for the calculated excess entropy ΔS ($\Delta H = 11\,\mathrm{cal\,mole^{-1}}$ and $\Delta S = 0.03\,\mathrm{cal\,mole^{-1}\,K^{-1}}$) which implies that only a small change in the structure may exists at that temperature.

For the elastic properties of KIO_3 single crystal as related to II–III transition, Haussühl *et al*. [24] found that, the shear stiffness C_{66}^{E} shows a drastic softening on approaching the transition temperature (345.6 K) from the lower temperature. This implies that this transition is a second order ferroelastic phase transition.

Among other things, the mentioned transition finds a strong support from Raman scattering. From their study of the optical soft modes responsible for the phase transition at 345 K (72°C) Ahart *et al*. [36] observed a remarkable softening towards II–III transition. Furthermore, detailed Raman study on KIO_3 single crystal performed recently [26] from 78.5 K–553 K shows two soft modes S_1 and S_2 which are related to II–III phase transition.

Regarding the crystal structure associated with II–III transition, although the transition from I–III was proposed to be the only structural transition in the temperature range 10–523 K according to neutron scattering [22], yet other authors proposed the existence of such a structural phase transition [18, 35]. According to ref. [35] phase II is monoclinic (*pm*, $z = 2$) and is also monoclinic but with C_{m} [18]. The present investigation support and confirm such transitions but the fall structure is beyond the scope of this work. Furthermore, Raman scattering results [26, 36] also support the existence of the I–II and II–III phase transitions in KIO_3 compound.

For further analysis of our data, we comment on the behaviour of s in the two models for the ac conductivity namely the QMT and the hopping over the barrier models [41]. For QMT, we have

$$s = 1 - \frac{4}{\ell n(\nu_{\mathrm{ph}}/\omega)}.$$

Whereas for hopping model, the value of s is given by:

$$s = 1 - \frac{6kT}{E_0 - kT\ell \mathrm{n}(1/\omega\tau_0)}.$$

The symbols take their usual meaning, $0 < s < 1$ in both models. The exponent s in the second model decreases with increasing temperature and is less dependent on

the frequency. This behaviour agrees quite well with the thermal features of s where its value decreases from about 0.75 at ≈ 345 K to 0.4 at ≈ 520 K. The hopping over the barrier model seems to be the more likely one for conduction mechanism in the present compound.

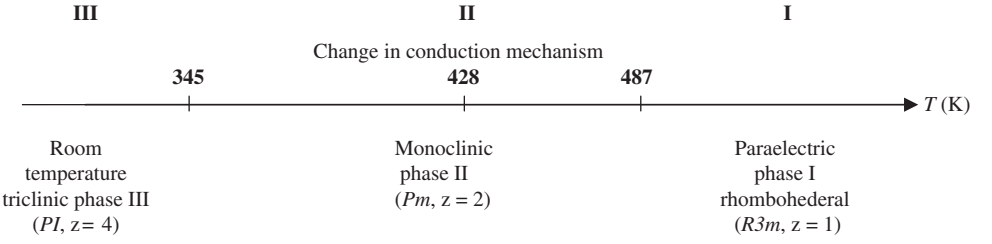

Conclusion

The results of the present work give the first electrical measurements that support and confirm the improper characteristic features of the KIO_3 compound which were proposed recently by Raman scattering experiments. Moreover, our data were discussed in the light of these features. The transition at (428 ± 2) K, which is usually detectable in some parameters and undetectable in the others, is most probably due to the change in the conduction mechanism rather than phase transition. The improper ferroelectric KIO_3 undergoes a ferroelectric phase transition (I–II) at (486 ± 1) K, whereas the second structural phase transition II–III (most probably associated with ferroelastic transition) was observed at (345 ± 2) K.

References

[1] J.M. Crettez, A. Righi, C. Galez, *et al.*, Sol. Stat. Comm. **105** 481 (1998).
[2] T. Oka and T. Mitsui, J. Phys. Soc. Jap. **40** 913 (1976).
[3] G.R. Crane, J.C. Bergman and A.M. Glass, J. Am. Ceramic Soc. **52** 655 (1969).
[4] G. Nath and S. Haussuhl, Appl. Phys. Lett. **14** 154 (1969).
[5] D.M. Hwang and S.A. Salin, Phys. Rev. B **7** 843 (1973).
[6] G.M. Loiacono and J.G. Jacco, Mater. Letters **4** 27 (1985).
[7] M.H. Brooker and J.G. Shapter, J. Phys. Chem. Sol. **50** 1087 (1989).
[8] V.K. Wadhawan, Acta Cryst. A **36,** 851 (1980).
[9] S. Haussuhl, Acta Cryst. A **33** 322 (1977).
[10] K. Viswanathan and E. Salje, Acta. Cryst. A **31** 810 (1975).
[11] M.A. Gaffar and A. Abu El-Fadl, J. Phys. Chem. Solids **60** 1633 (1999).
[12] F.E.A. Melo, F. Cerdeira and V. Lemos, Sol. Stat. Comm. **41** 281 (1982).
[13] J.M. Crettez, E. Coquet, B. Michaux, *et al.*, Physica B+C **144** 277 (1987).
[14] F. Herlach, Helv. Phys. Acta **34** 305 (1961).
[15] E. Salje, Z. Kristallogr. **134** 107 (1971).
[16] U. Helg, Z. Kristallogr. **131** 241 (1970).
[17] N.R. Ivanov, L.A. Shuvalov and O.A. Chikhladze, Phys. Letters **45A** 437 (1973).
[18] G.R. Crane, J. Appl. Cryst. **5** 360 (1972).
[19] V.R. Kalinin, V.V. Llyukhin and N.V. Belov, Sov. Phys. Dokl. **12** 1978 (1978).
[20] H. Kasatani, S. Aoyagi, Y. Kuroiwa, *et al.*, Nucl. Instr. Meth. B **199** 49 (2003).
[21] B.W. Lucas, Acta Cryst. C **40** 1989 (1984).

[22] P.G. Byrom and B.W. Lucas, Acta Cryst. C **43** 1651 (1987).
[23] X. Yin and M.K. Lü, App. Phys. Lett. **60** 2849 (1992).
[24] S. Haussühl, W. Jyang and L. Mengkai, Cryst. Res. Technology **30** 535 (1995).
[25] M. Maeda, M. Takagi and I. Suzuki, J. Phys. Soc. Jpn. **69** 267 (2000).
[26] L. Liu, R.Q. Wu, Z.H. Ni, *et al*., J. Phys. Conf. Ser. **28** 105 (2006).
[27] M.M. Abdel-Kader, M.M. Mosaad, M.A. Fahim, *et al*., Phase Trans. **62** 105 (1997).
[28] M.M. Abdel-Kader, H.M. Naguib, H.M. Abdel-Monem et al., Phase Trans. 78 621 (2005) and references there in.
[29] M.M. Abdel-Kader, M. Fadly, M. Abutaleb, *et al*., Physica Scripta **52** 334 (1995).
[30] M.F. Mostafa, M.M. Abdel-Kader, S.S. Arafat, Z. Naturforsch. **57A** 897 (2002) and references there in.
[31] W.K. Lee, J.F. Liu and A.S. Nowick, Phys. Rev. Lett. **67** 1559 (1991).
[32] A.K. Jonsher, *Dielectric Relaxation in Solids* (Chelsea Dielectric press, London, 1983), p. 223.
[33] A. Pradel and M. Ribes, J. Non-Cryst. Solids **131**–**133** 1063 (1991).
[34] J.C. Dyre, J. Appl. Phys. **64** 2456 (1988).
[35] E. Salje, Z. Kristallogr. **139** 317 (1974).
[36] M. Ahart, S. Kojma, M. Takagi, *et al*., Jpn. J. Appl. Phys. **37** 5687 (1998).
[37] R. Blinc, B. Zeks, Soft Modes in Ferroelectrics and Anti Ferroelectrics, Vol. XIII (North Holland Pub. Co., Amsterdam, 1974) P. 15, 45.
[38] B.A. Strukov and A.P. Levanyuk, *Ferroelectric Phenomena in Crystals* (Springer Berlin, 1998), p. 74.
[39] T. Shigenari, Y. Takagi and Y. Wakabayashi., Solid State Commun. **18** 1271 (1976).
[40] L.E. Cross, A. Fouskova and S.E. Cummins, Phys. Rev. Lett. **21** 812 (1968).
[41] S.R. Elliott, Adv. Phys. **36** 135 (1987).